Long-lived quasinormal modes and overtones' behavior of holonomy-corrected black holes

S. V. Bolokhov*

Peoples' Friendship University of Russia (RUDN University), 6 Miklukho-Maklaya Street, Moscow 117198, Russia

(Received 26 November 2023; accepted 5 June 2024; published 8 July 2024)

Recently massless test scalar field perturbations of the holonomy-corrected black holes [Z. S. Moreira *et al.*, Quasinormal modes of a holonomy corrected Schwarzschild black hole, Phys. Rev. D **107**, 104016 (2023).] were studied in order to estimate quantum corrections to the quasinormal spectrum of a black hole. Here we study both the fundamental mode and overtones of scalar, electromagnetic and Dirac fields with the help of the Leaver method and higher-order WKB formula with Padé approximants. We observe that the overtones depend on the geometry near the event horizon, while the fundamental mode is localized near the peak of the potential barrier, what agrees with previous studies. We showed that unlike a massless field, the massive one possesses arbitrarily long-lived modes. We also obtain the analytical eikonal formula for quasinormal modes and its extension beyond eikonal approximation as a series in powers of $1/\ell$, where ℓ is the multipole number.

DOI: 10.1103/PhysRevD.110.024010

I. INTRODUCTION

Quasinormal modes of black holes are crucial phenomena in the field of astrophysics and general relativity. These modes represent the characteristic oscillations that arise when perturbations are introduced to a black hole [1–4]. They are essential for comprehending the fundamental properties of black holes, including their mass, spin, and charge, as they manifest through the distinct frequencies and damping times of these modes.

The study of quasinormal modes is imperative for scientists as it enables a deeper examination of black hole structure and offers a means to test the predictions of Einstein's theory of general relativity in the strong field regime. These modes serve as indispensable tools for gravitational wave astronomy, allowing for the detection and analysis of black hole mergers through the gravitational waves they emit [5,6]. Moreover, quasinormal modes are instrumental in investigating the possibility of exotic black hole solutions, including those that arise from modifications to general relativity or theories involving extra dimensions (see, for instance, [7–14] and references therein).

Furthermore, quasinormal modes provide a unique avenue to probe quantum gravity effects near black holes. In summary, quasinormal modes of black holes are pivotal in advancing our understanding of the fundamental nature of black holes, while also serving as a means to test the boundaries of quantum gravity.

*bolokhov-sv@rudn.ru

A particular black hole model we are interested in here is suggested in [15,16] and motivated by the holonomy corrections owing to quantum gravity. Various properties of these black holes have been recently studied in [17,18], while the first study of the quasinormal spectrum of the massless scalar and electromagnetic fields was done in [19] with the WKB and time-domain integration methods with the emphasis on the eikonal limit. A more detailed and accurate study of a test massless scalar field with the help of the lower order WKB method and Frobenius approach was done in [20].

Here we make the next step and study in detail quasinormal frequencies of scalar (both massless and massive), electromagnetic and Dirac fields in the vicinity of such black holes with the help of the accurate convergent Frobenius method and check them with the higher-order WKB method with Padé approximants. We will pay special attention to the two aspects of the quasinormal spectrum: arbitrary long-lived modes which take place for massive fields [21,22] and overtones behavior. The overtones are important, because they are necessary to reproduce the ringdown signal not only at the late stage, but at the beginning of the ringing as well [23,24]. The massive term appears as an effective term in various higher dimensional scenarios [9,25] and when introducing magnetic fields around black holes [26,27]. Among other observations, we will show that the first few overtones deviate from their Schwarzschild limit at a smaller rate than the fundamental mode, while at sufficient high n the situation is opposite: the overtones differ from the Schwarzschild ones more than the fundamental mode $n = 0$. We will show that this

behavior is supported by the claim made in [28], that the overtones are determined mainly by the geometry near the event horizon, while the fundamental mode is fixed by the scattering properties near the peak of the effective potential, which is at some distance from the black hole.

The paper is organized as follows. In Sec. II we briefly describe the holonomy-corrected black hole, which is the main object under consideration. Section III is devoted to the general setup related to the background metric, wave equations and boundary conditions. Section IV is a brief summary on the methods used for finding quasinormal modes: Frobenius method, higher-order WKB approach with Padé approximants and the time-domain integration. Section V relates the results to numerical calculations of quasinormal modes, while Sec. VI is about analytical formulas for quasinormal modes in the eikonal limit and beyond it.

II. HOLONOMY-CORRECTED BLACK HOLE

There is a well-founded belief that the general relativity (GR) is not a final theory of gravity and should be replaced by a more fundamental theory usually referred to as quantum gravity, which is expected to give more precise description of quantized space-time on the Planck scales and resolve a number of problems (such as cosmological or black hole singularities) where the classical GR description fails due to a crucial role of quantum effects in large-curvature regions. There is a well-known class of approaches to construct such a theory within the framework of Loop Quantum Gravity. Difficulties with standard canonical quantization scheme led to the discovery of a possibility to reformulate GR in terms of suitable canonical variables (so-called Ashtekar-Barbero's variables) and to construct a class of effective models by using appropriate deformations of the GR Hamiltonian constraint (a "polymerization technique"). It can also be understood in a geometrical fashion in terms of the corrections to the holonomy of a connection.

One such deformation scheme was considered in [15,16], where a dimensionless deformation parameter λ was introduced, effectively encoding a measure of discretization of the quantum space-time. GR is recovered in the limiting case $\lambda \to 0$. The corresponding deformed and regularized Hamiltonian leads to an effective theory which admits the following static, spherically symmetric, and asymptotically flat background metric:

$$ds^2 = (1-2M/r)dt^2 + \frac{dr^2}{(1-r_0/r)(1-2M/r)} + r^2(d\theta^2+\sin^2\theta d\phi^2). \quad (1)$$

This metric has a horizon at $r_h = 2M$ and therefore can be considered as a holonomy-corrected black hole (BH). The correction is governed by a parameter $r_0 \equiv 2M\lambda^2/(1+\lambda^2)$, which has the meaning of a quantum characteristic scale. One can see from its definition that $0 \le r_0 < 2M$, whereas the case $r_0 \to 0$ leads to the Schwarzschild metric.

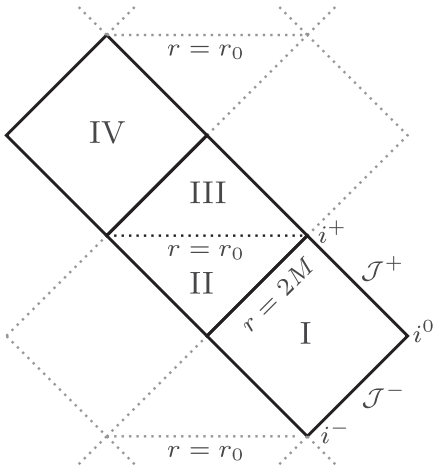

FIG. 1. Penrose diagram of a maximally extended space-time corresponding to metric (1) with the transition hypersurface $r = r_0$ between BH and white hole regions, according to [16].

The parameter r_0 is always less than r_h and therefore defines geometric features of the space-time in the inner (nonstatic) BH region. A detailed analysis of the global causal structure of metric (1) performed in [15] shows that there is a bounce at the transition hypersurface $r = r_0$ (see Fig. 1), which separates the black and white hole regions of the maximally extended space-time. The value r_0^2 determines minimal area of coordinate spheres in such a geometry, keeping all curvature invariants finite. Thus, the metric (1) is quite an elegant example of a regular quantum-corrected BH with nontrivial bouncing behavior and a natural GR limit to the Schwarzschild solution.

III. GENERAL SETUP

Given a general spherically symmetric BH with the metric

$$ds^2 = -A(r)dt^2 + B(r)dr^2 + r^2(d\theta^2+\sin^2\theta d\phi^2), \quad (2)$$

we have the following general expressions for effective potentials of scalar, electromagnetic and Dirac fields respectively:

$$V_{\rm sc}(r) = A(r)\frac{\ell(\ell+1)}{r^2} + \frac{1}{2r}\frac{d}{dr}\frac{A(r)}{B(r)} + A(r)\mu^2, \quad (3)$$

$$V_{\rm em}(r) = A(r)\frac{\ell(\ell+1)}{r^2}, \quad (4)$$

$$V_{\rm D\pm}(r) = \frac{A(r)k^2}{r^2} \mp \frac{A(r)k}{r^2\sqrt{B(r)}} \pm \frac{kA'(r)}{2r\sqrt{B(r)}}, \quad (5)$$

where the multipole numbers $\ell = 0, 1, 2, 3\ldots$ for the scalar field, $\ell = 1, 2, 3\ldots$ for electromagnetic field, and $k = 1, 2, 3, \ldots$ for the Dirac field. The quantity μ is the mass of the scalar field. Here the coordinate r is supposed to be a function of the "tortoise" coordinate r_* via the relation

$$dr_* = \frac{dr}{f(r)}, \qquad f(r) \equiv \sqrt{A(r)/B(r)}. \tag{6}$$

The general master equation for calculating quasinormal modes (QNM) ω has the form [1]

$$\frac{d^2\Psi}{dr_*^2} + (\omega^2 - V(r))\Psi = 0 \tag{7}$$

with the standard boundary conditions for the QNM problem, which are a requirement of purely incoming waves at the event horizon and purely outgoing ones at infinity.

In our case the metric functions from Eq. (1) have the form

$$A(r) = 1 - 2M/r, \qquad B(r) = \frac{1}{(1 - r_0/r)A(r)}. \tag{8}$$

Choosing $M = 1/2$ we have the normalized horizon radius $r_h = 1$.

The effective potentials for massless fields have the form of positive definite potential barriers with a single maximum (see Figs. 2 and 3), except one of the chiralities of the Dirac case, for which a negative gap near the event horizon takes place, as shown in Fig. 3. However, the potential with the gap is isospectral with the other chirality case, so that it is sufficient to consider only one of the chiralities.

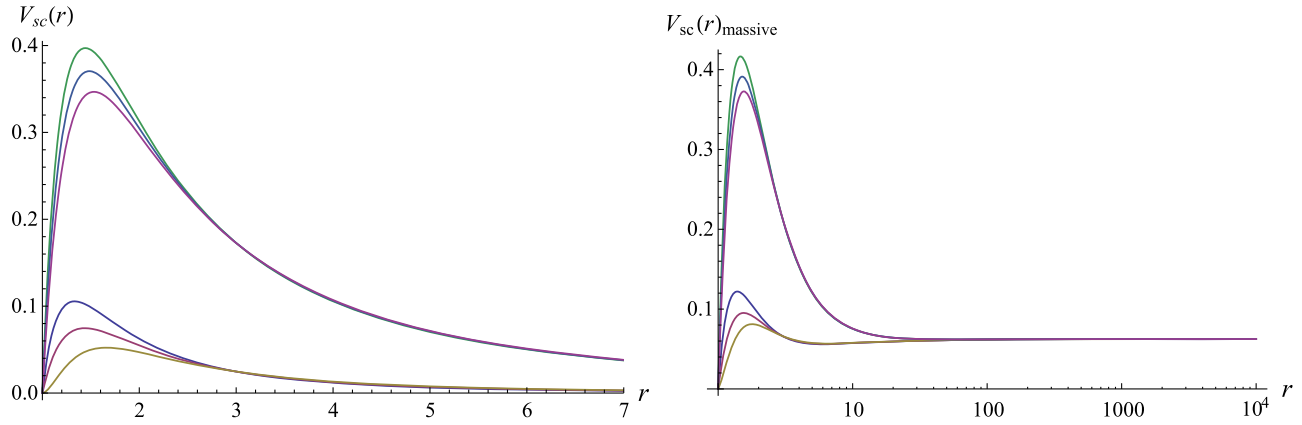

FIG. 2. Left panel: effective potentials of a massless scalar field for $\ell = 0$ (bottom bundle of curves, $r_0 = 0$, 0.5, 0.99 from top to bottom) and $\ell = 1$ (top bundle of curves, $r_0 = 0$, 0.5, 0.99 from top to bottom), $r_h = 1$. Right panel: effective potential of a massive scalar field for $\mu = 0.25$, $\ell = 0$ (bottom bundle of curves, $r_0 = 0$, 0.5, 0.99 from top to bottom) and $\ell = 1$ (top bundle of curves, $r_0 = 0$, 0.5, 0.99 from top to bottom), $r_h = 1$.

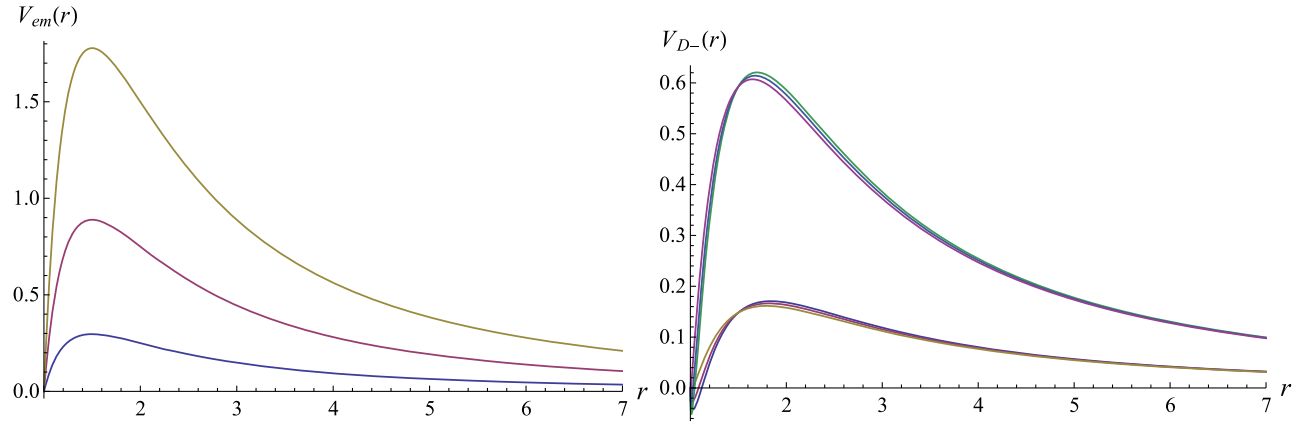

FIG. 3. Left panel: effective potentials of electromagnetic field for $\ell = 1$, 2, 3 (from bottom to top), $r_h = 1$. Right panel: effective potential $V_{D-}(r)$ of the Dirac field for $k = 1$ (bottom bundle of curves, $r_0 = 0.1$, 0.5, 0.9 from top to bottom), and $k = 2$ (top bundle of curves, $r_0 = 0.1$, 0.5, 0.9 from top to bottom), $r_h = 1$.

The massive term complicates the shape of the potential as shown in Fig. 2.

IV. WKB AND FROBENIUS METHODS FOR QNMS

Both methods used here are discussed in a great number of works. Therefore, here we will briefly summarize these methods, while further details can be found in [1,29].

A. Frobenius method

To acquire precise values of quasinormal modes, including overtones with $\ell < n$, we will employ the Frobenius method, also known as the Leaver method [30]. The main point of the method is that the solution to the second order differential equation can be expanded into a Frobenius series around the regular singular point. It is required that the coefficients in the wave equation have polynomial form, so that it can be applied to the scalar and electromagnetic fields, but not to the Dirac field in the representation we used here. The master wavelike differential equation has a regular singular point at the event horizon $r = r_h$, and an irregular one at $r = \infty$. Therefore, similar to the approach in [31], we introduce a novel wave function:

$$\Psi(r) = P(r,\omega)\left(1-\frac{r_h}{r}\right)^{-i\omega/F'(r_h)} y(r), \tag{9}$$

where we choose $P(r,\omega)$ in such a way that $y(r)$ is regular in the interval $r_h \le r < \infty$, ensuring that $\Psi(r)$ complies with the quasinormal mode boundary conditions, which require purely incoming waves at the event horizon and purely outgoing waves at infinity. Subsequently, we express $y(r)$ in terms of a Frobenius series as follows:

$$y(r) = \sum_{k=0}^{\infty} a_k \left(1-\frac{r_h}{r}\right)^k. \tag{10}$$

In order to find the coefficients a_k quickly in the above expansion we apply Gaussian elimination to the recurrence relation governing the expansion coefficients. This way the problem is simplified to a solution of an algebraic equation depending on ω. We will also use the Nollert improvement [32] in the general n-term recurrence relation form [33] in order to speed up the convergence of the procedure. When singular points of the wavelike equation are located inside the unit circle $|x| < 1$, we employ integration through a series of positive real midpoints as was suggested in [34].

B. WKB approach

The semianalytic WKB approach was applied for the first time by [35] to find quasinormal frequencies of asymptotically flat black holes. Then, the first order formula of [35] was extended to higher orders in subsequent papers [36–38] and seemingly improved by using the Padé approximants [38,39].

The general form of the WKB formula can be written symbolically as an expansion around the first order, eikonal limit [29]:

$$\omega^2 = V_0 + A_2(\mathcal{K}^2) + A_4(\mathcal{K}^2) + A_6(\mathcal{K}^2) + \ldots - i\mathcal{K}\sqrt{-2V_2}(1 + A_3(\mathcal{K}^2) + A_5(\mathcal{K}^2) + A_7(\mathcal{K}^2) + \ldots), \tag{11}$$

where $\mathcal{K} = n + 1/2$ is half integer. The corrections $A_k(\mathcal{K}^2)$, of order k, in the eikonal formula are polynomials of $\mathcal{K}^2$ with rational coefficients. The explicit form of these correction terms at various WKB orders is written in the above works [36–38].

These corrections are contingent upon the values of higher-order derivatives of the effective potential $V(r)$ at its maximum, denoted as V_j, $(j = 0, 1, 2, \ldots)$. In order to enhance the precision of the WKB formula, we employed the aforementioned approach presented by Matyjasek and Opala [38], which utilizes Padé approximants. Specifically, we utilized the sixth-order WKB technique with $\tilde{m} = 5$, where $\tilde{m}$ signifies the corresponding polynomial degrees within the expressions for Padé approximants [29,38]. This selection provides the most accurate results in the Schwarzschild limit. Usually when the WKB frequency does not change much when one changes the WKB order or the Padé splitting, say, fifth or sixth orders with $\tilde{m} = 4$ or 5 lead to almost the same frequencies, then this WKB result is usually in a very good agreement with the precise values (see, for example, [40–42]). Thus, we use this "plateau of relative convergence" as an indicator of trusting to the WKB results.

However it is crucial to emphasize that the convergence of the WKB series is purely asymptotic and the WKB method does not guarantee increased precision at each order. Additionally, it does not insure the precise calculation of $\ell < n$ overtones, though in some cases the first few such overtones could be found with reasonable accuracy. Therefore, in this context, we will employ the WKB method mainly as an additional check for the Leaver method when dealing with the fundamental mode $n = 0$ and also in order to find an initial guess for the frequency which can be calculated precisely with the Leaver method.

V. TIME-DOMAIN INTEGRATION

One can study evolution of perturbations in the time domain using the integration of the wavelike equation at a fixed point in space. For this we use the null-cone variables

$u = t - r_*$ and $v = t + r_*$ and apply the Gundlach-Price-Pullin discretization scheme suggested in [43]:

$$\Psi(N) = \Psi(W) + \Psi(E) - \Psi(S) - \Delta^2 V(S)\frac{\Psi(W) + \Psi(E)}{4} + \mathcal{O}(\Delta^4). \tag{12}$$

Here, the designation of the points are the following: $N \equiv (u + \Delta, v + \Delta)$, $W \equiv (u + \Delta, v)$, $E \equiv (u, v + \Delta)$, and $S \equiv (u, v)$. This method has also been used for finding quasinormal modes and testing the stability of perturbations in a great number of works (see, for example, [42,44–47] for recent references) and showed very good concordance with other methods in the common range of applicability.

VI. QUASINORMAL MODES

A. Scalar field case

Quasinormal modes for the scalar field will be considered here for both massless and the massive case. As can be seen from Tables I–III, the frequencies obtained by the sixth order WKB with the Padé approximants are quite close to the accurate Frobenius data, keeping the error within a small fraction of one percentage, except the quasiextreme case, for which the relative error in the damping rate achieves 1%. Results obtained by the usual sixth (here) and third (in [20]) order WKB method are much less accurate, while the time-domain integration does not allow one to extract frequency with sufficient accuracy at $\ell = 0$ perturbations [19]. The results for massless scalar field perturbations are also graphically represented in Fig. 4. We can see that both the real oscillation frequency and the damping rate decrease as the quantum correction parameter is increased. The damping rate is much more sensitive to the change of r_0 than the $\mathrm{Re}(\omega)$.

When the mass term μ is tuned on, the damping rate monotonically decreases, so that there is a clear indication of the arbitrarily long-lived modes, called quasiresonances (see Figs. 5 and 6). The existence of such modes is not guaranteed for every background. For example, they are not allowed for the Schwarzschild-de Sitter space-time [48].

An interesting aspect is related to the behavior of overtones shown in Table IV: while the fundamental mode

TABLE I. WKB QNMs of the massless scalar field for $n = 0$, $\ell = 0$ and various r_0. The relative errors between the Frobenius and WKB6(Pade) data are denoted by δ_{Re} and δ_{Im}.

r_0	6WKB	6WKB(Pade6)	Frobenuis	δ_{Re}, %	δ_{Im}, %
0	0.220934–0.201633 i	0.221357–0.208847 i	0.220910–0.209791 i	0.2	0.5
0.1	0.217552–0.193567 i	0.217915–0.200040 i	0.217504–0.200937 i	0.2	0.4
0.2	0.213934–0.185853 i	0.214249–0.191100 i	0.213874–0.191970 i	0.2	0.5
0.3	0.210448–0.178204 i	0.210136–0.182227 i	0.209951–0.182897 i	0.09	0.4
0.4	0.208655–0.167544 i	0.205219–0.173611 i	0.205638–0.173735 i	0.2	0.07
0.5	0.208603–0.151038 i	0.200411–0.164719 i	0.200799–0.164527 i	0.2	0.1
0.6	0.203865–0.134380 i	0.196607–0.155284 i	0.195235–0.155375 i	0.7	0.06
0.7	0.190388–0.126561 i	0.189317–0.142897 i	0.188651–0.146532 i	0.4	2
0.8	0.177940–0.124934 i	0.179155–0.136701 i	0.180457–0.138822 i	0.7	2
0.9	0.171056–0.122278 i	0.172101–0.132516 i	0.172187–0.133779 i	0.05	0.9
0.99	0.166036–0.118817 i	0.166942–0.128819 i	0.166989–0.130381 i	0.03	1

TABLE II. WKB QNMs of the massless scalar field for $n = 0$, $\ell = 1$ and various r_0. The relative errors between the Frobenius and WKB6(Pade) data are denoted by δ_{Re} and δ_{Im}.

r_0	6WKB	6WKB(Pade6)	Frobenius	δ_{Re}, %	δ_{Im}, %
0	0.585819–0.195523 i	0.585864–0.195320 i	0.585872–0.195320 i	0.001	0.0002
0.1	0.584762–0.188491 i	0.584783–0.188359 i	0.584781–0.188354 i	0.0003	0.003
0.2	0.583633–0.181290 i	0.583644–0.181190 i	0.583630–0.181193 i	0.002	0.001
0.3	0.582424–0.173882 i	0.582414–0.173797 i	0.582405–0.173811 i	0.002	0.008
0.4	0.581117–0.166233 i	0.581089–0.166167 i	0.581087–0.166180 i	0.0003	0.008
0.5	0.579685–0.158305 i	0.579648–0.158255 i	0.579649–0.158265 i	0.0002	0.006
0.6	0.578086–0.150056 i	0.578050–0.150017 i	0.578052–0.150023 i	0.0003	0.004
0.7	0.576262–0.141436 i	0.576234–0.141402 i	0.576235–0.141405 i	0.0002	0.002
0.8	0.574121–0.132394 i	0.574107–0.132354 i	0.574273–0.131821 i	0.03	0.4
0.9	0.571523–0.122887 i	0.571527–0.122835 i	0.571522–0.122834 i	0.0008	0.0006
0.99	0.568621–0.113936 i	0.568634–0.113865 i	0.568635–0.113867 i	0.0001	0.002

TABLE III. WKB QNMs of the massless scalar field for $n = 0$, $\ell = 2$ and various r_0. The relative errors between the Frobenius and WKB6 (Pade) data are denoted by δ_{Re} and δ_{Im}.

r_0	6WKB	6WKB(Pade6)	Frobenuis	δ_{Re}, %	δ_{Im}, %
0	0.967284–0.193532 i	0.967287–0.193518 i	0.967288–0.193518 i	0.0001	0.0001
0.1	0.966641–0.186843 i	0.966643–0.186830 i	0.966644–0.186830 i	0.00007	0.0001
0.2	0.965963–0.179931 i	0.965965–0.179920 i	0.965965–0.179920 i	0.00004	0.0001
0.3	0.965243–0.172771 i	0.965244–0.172761 i	0.965244–0.172761 i	0.00002	0.0001
0.4	0.964467–0.165328 i	0.964467–0.165320 i	0.964467–0.165320 i	$7.\times10^{-6}$	0.0001
0.5	0.963619–0.157565 i	0.963619–0.157558 i	0.963619–0.157558 i	0.00002	0.00008
0.6	0.962675–0.149431 i	0.962675–0.149425 i	0.962675–0.149425 i	0.00003	0.00004
0.7	0.961598–0.140865 i	0.961598–0.140860 i	0.961598–0.140860 i	0.00003	0.00001
0.8	0.960332–0.131789 i	0.960332–0.131785 i	0.963197–0.130726 i	0.3	0.8
0.9	0.958783–0.122110 i	0.958784–0.122106 i	0.958783–0.122106 i	0.00002	0.00007
0.99	0.957022–0.112793 i	0.957022–0.112790 i	0.957022–0.112790 i	$9.\times10^{-6}$	0.00008

deviates from its Schwarzschild limit seemingly, by 1.6%, the first few overtones change at a much smaller, but increasing with n rate, so that at higher n the situation becomes the opposite, i.e., the overtones deviate from their classical limits much more than the fundamental mode. This behavior agrees with observation made in [28,49], which says that while the fundamental mode is determined by the geometry near the peak of the effective potential,

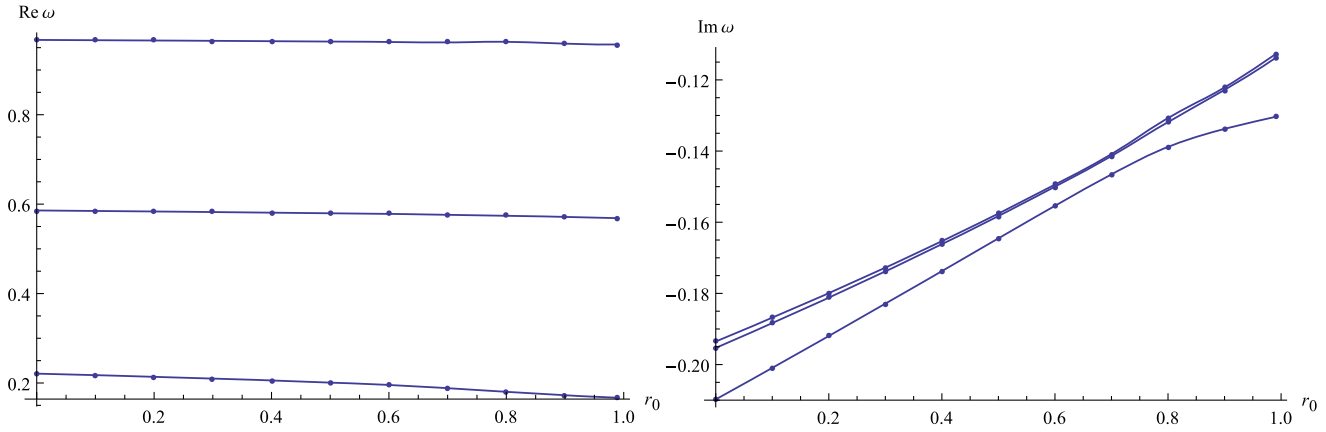

FIG. 4. The modes $n = 0$, $\ell = 0$, 1, 2 (from bottom to top) for massless scalar field perturbations as functions of r_0.

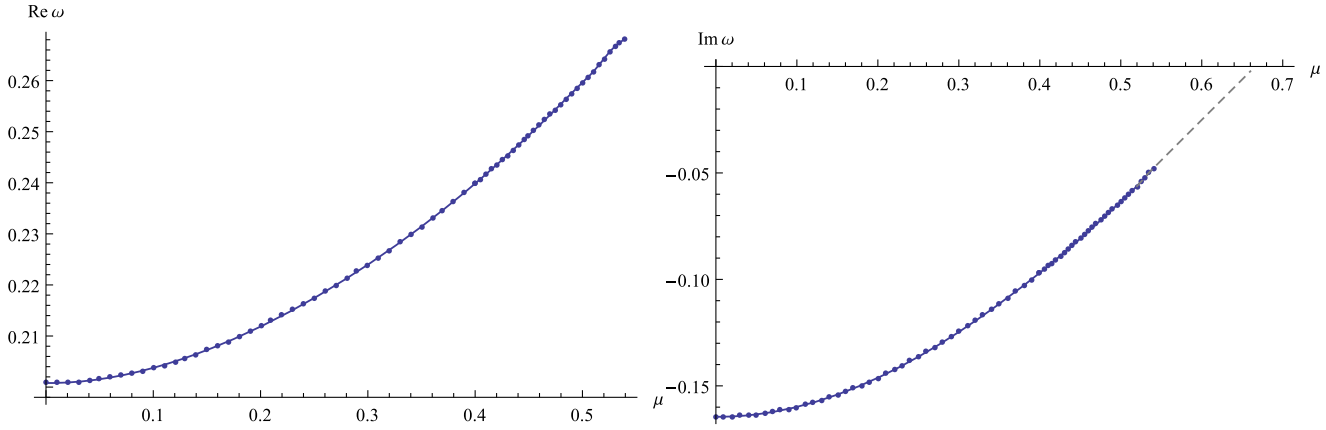

FIG. 5. The real and imaginary parts of the fundamental mode $n = 0$, $\ell = 0$ as functions of the mass μ, obtained by the Frobenius method for a massive scalar field in case $r_0 = 0.5$. The dotted lines represent numerical data, whereas the dashed line is an extrapolation curve indicating the quasiresonant behavior.

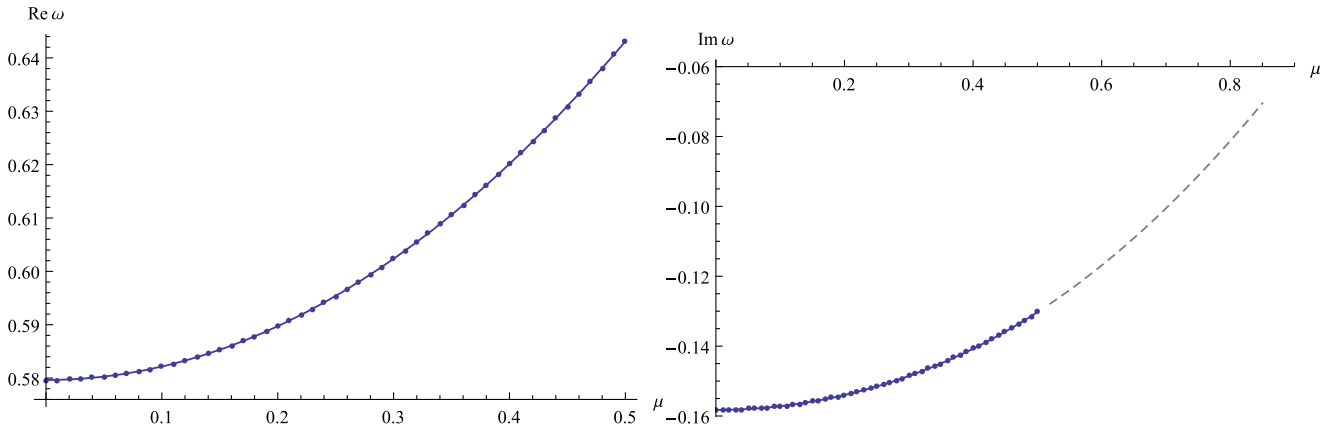

FIG. 6. The real and imaginary parts of the fundamental mode $n = 0$, $\ell = 1$ as functions of the mass μ, obtained by the Frobenius method for a massive scalar field in case $r_0 = 0.5$. The dotted lines represent numerical data, whereas the dashed line is an extrapolation curve indicating the quasiresonant behavior.

the overtones are determined by the geometry in the near-horizon zone. Indeed, the effective potentials (see Figs. 2 and 3) strongly deviate from the Schwarzschild ones near the maximum, but only slightly near the horizon. Therefore, the fundamental mode deviates a lot, while the first few overtones deviate at a smaller rate, though, since the phenomenon called "outburst of overtones" [28] takes place even at small deformation in the near-horizon zone, the rate of deviation increases with n, so that at sufficiently high n the frequencies differ much more from the Schwarzschild ones than the fundamental mode.

TABLE IV. QNMs of massless scalar field for the holonomy-corrected BH ($r_0 = 0.1$, the Frobenius method) and the Schwarzschild BH ($r_0 = 0$) for $\ell = 0$ and various overtones n. The relative difference for Reω between these two cases is denoted by δ_{Re}.

n	Holonomy-corrected BH	Schwarzschild BH	δ_{Re}, %
0	0.217504–0.200937 i	0.220910–0.209791 i	1.6
1	0.172460–0.664156 i	0.172234–0.696105 i	0.1
2	0.153352–1.145927 i	0.151484–1.202157 i	1.2
3	0.143758–1.626790 i	0.140820–1.707355 i	2.0
4	0.137896–2.106328 i	0.134149–2.211264 i	2.7
5	0.133881–2.584943 i	0.129483–2.714279 i	3.3
6	0.130922–3.062923 i	0.125988–3.216683 i	3.8
7	0.128627–3.540451 i	0.123242–3.718654 i	4.2
8	0.126777–4.017645 i	0.121013–4.220307 i	4.5
9	0.125240–4.494585 i	0.119154–4.721719 i	4.9

B. Electromagnetic field case

For electromagnetic perturbations there are some distinctions from the scalar case. The results are represented in Tables V–VII and Fig. 7. First of all, Re(ω) monotonically increases as r_0 is increased, unlike the scalar case, for which it monotonically decreases. As $\ell = 1$ is the minimal value of the multipole number now, the accuracy of the WKB method with Padé approximants is really great now as the comparison with the accurate Frobenius data in Tables V–VI shows. An important difference with the scalar case is connected to the overtones' behavior and can be easily explained. The overtones deviate from the Schwarzschild values at a higher rate than the fundamental

TABLE V. WKB QNMs of electromagnetic field for $n = 0$, $\ell = 1$ and various r_0. The relative errors between the Frobenius and WKB6 (Pade) data are denoted by δ_{Re} and δ_{Im}.

r_0	6WKB	6WKB(Pade6)	Frobenuis	δ_{Re}, %	δ_{Im}, %
0	0.496383–0.185274 i	0.496509–0.184961 i	0.496527–0.184975 i	0.004	0.008
0.1	0.499896–0.179638 i	0.500019–0.179280 i	0.500035–0.179291 i	0.003	0.007
0.2	0.503368–0.173640 i	0.503482–0.173268 i	0.503496–0.173276 i	0.003	0.005
0.3	0.506777–0.167250 i	0.506879–0.166889 i	0.506890–0.166895 i	0.002	0.004
0.4	0.510100–0.160433 i	0.510186–0.160101 i	0.510195–0.160105 i	0.002	0.003
0.5	0.513301–0.153142 i	0.513371–0.152852 i	0.513377–0.152855 i	0.001	0.002
0.6	0.516331–0.145320 i	0.516383–0.145079 i	0.516387–0.145079 i	0.0007	0.0003
0.7	0.519115–0.136893 i	0.519150–0.136703 i	0.519151–0.136701 i	0.0003	0.002
0.8	0.521532–0.127774 i	0.521552–0.127634 i	0.521732–0.126988 i	0.03	0.5
0.9	0.523386–0.117876 i	0.523396–0.117779 i	0.523384–0.117771 i	0.002	0.008
0.99	0.524316–0.108278 i	0.524322–0.108206 i	0.524295–0.108205 i	0.005	0.0008

TABLE VI. WKB QNMs of electromagnetic field for $n = 0$, $\ell = 2$ and various r_0. The relative errors between the Frobenius and WKB6 (Pade) data are denoted by δ_{Re} and δ_{Im}.

r_0	6WKB	6WKB(Pade6)	Frobenuis	δ_{Re}, %	δ_{Im}, %
0	0.915187–0.190022 i	0.915190–0.190009 i	0.915191–0.190009 i	0.0001	0.0001
0.1	0.917186–0.183746 i	0.917189–0.183731 i	0.917190–0.183731 i	0.0001	0.0001
0.2	0.919149–0.177203 i	0.919152–0.177188 i	0.919152–0.177188 i	0.00008	0.0001
0.3	0.921067–0.170365 i	0.921070–0.170351 i	0.921070–0.170350 i	0.00006	0.00009
0.4	0.922928–0.163195 i	0.922930–0.163182 i	0.922931–0.163182 i	0.00005	0.00008
0.5	0.924714–0.155649 i	0.924716–0.155637 i	0.924716–0.155637 i	0.00003	0.00007
0.6	0.926399–0.147669 i	0.926401–0.147660 i	0.926401–0.147659 i	0.00001	0.00007
0.7	0.927945–0.139187 i	0.927946–0.139179 i	0.927946–0.139179 i	$8. \times 10^{-6}$	0.00007
0.8	0.929290–0.130111 i	0.929291–0.130105 i	0.930496–0.128371 i	0.1	1
0.9	0.930333–0.120328 i	0.930333–0.120325 i	0.930332–0.120325 i	0.00009	0.00009
0.99	0.930868–0.110811 i	0.930868–0.110808 i	0.930867–0.110809 i	0.0001	0.0007

mode already starting from the first overtone, though this deviation develops slowly, because for a chosen value of the parameters the difference in the geometry near the event horizon is quite small. The effective potential as a function of r is not affected by r_0 at all, and the difference in geometries of the Schwarzschild and holonomy-corrected black hole is encoded in the tortoise coordinate only. For larger values of r_0 the difference of the overtones values grows much quicker with n.

C. Dirac field case

For the Dirac field the effective potentials do not have a polynomial form, so that we will find quasinormal modes with the sixth order WKB formula with and without Padé approximants. As for scalar and vector fields the sixth order formula with Padé approximants provided very good concordance with the precise values; we believe that the same must be for the Dirac case for which the main condition of the applicability of the WKB method $\ell > n$ is fulfilled for the fundamental mode. The results of calculations are shown in Tables VIII and IX and in Fig. 8. There we can see that there is a nonmonotonic, but smooth change of $\mathrm{Re}(\omega)$ which first grows and then decays as r_0 is increased.

For the case of the Dirac field, square roots in the wave equation do not allow one to apply the Leaver method immediately. We apply the time-domain integration method for an additional check of the results obtained by the WKB method with Padé approximants. The results show the expected correspondence up to an accuracy of about fractions of one percentage, which becomes better when increasing k. The effect of the deviation from the Schwarzschild limit is clearly manifested in a decreasing damping rate as a function of r_0.

VII. ANALYTICAL FORMULA FOR QNMS IN THE EIKONAL LIMIT AND BEYOND

The regime of high real oscillation frequency, i.e., of high multipole numbers ℓ will hardly be observed in the near future, because in a merger of two compact objects such as black holes or neutron stars usually only a couple of first gravitational multipole numbers ($\ell = 2, 3$) are excited considerably. Nevertheless, there are a number of reasons of theoretical character to study this regime. First of all,

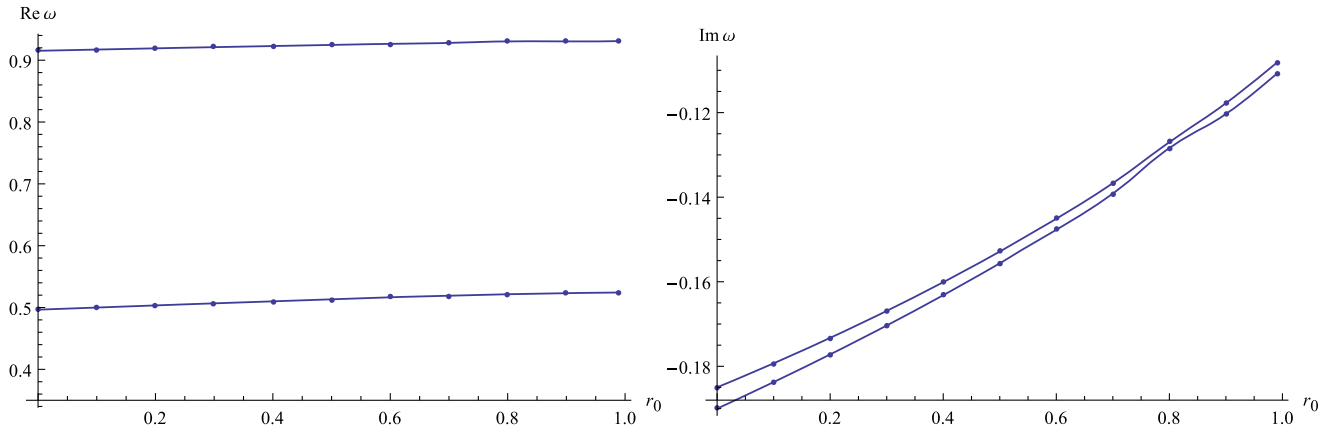

FIG. 7. The modes $n = 0$, $\ell = 1, 2$ (from bottom to top) for the electromagnetic field perturbations as functions of r_0.

TABLE VII. QNMs of electromagnetic field for the holonomy-corrected BH ($r_0 = 0.1$, the Frobenius method) and the Schwarzschild BH ($r_0 = 0$) for $\ell = 1$ and various overtones n. The relative difference for Reω between these two cases is denoted by δ_{Re}.

n	Holonomy-corrected BH	Schwarzschild BH	δ_{Re}, %
0	0.500035–0.179291 i	0.496527–0.184975 i	0.7
1	0.439399–0.566668 i	0.429031–0.587335 i	2.4
2	0.366907–1.008246 i	0.349547–1.050375 i	4.7
3	0.313786–1.478207 i	0.292353–1.543818 i	6.8
4	0.277119–1.955922 i	0.253108–2.045101 i	8.7
5	0.250381–2.435159 i	0.224506–2.547851 i	10.3
6	0.229739–2.914343 i	0.202429–3.050533 i	11.9
7	0.213084–3.393104 i	0.184647–3.552798 i	13.3
8	0.199192–3.871396 i	0.169870–4.054612 i	14.7
9	0.187310–4.349255 i	0.157299–4.556018 i	16.0

the eikonal regime corresponds to the limit of geometrical optics, and it comes as no surprise that in this regime there is a correspondence between characteristics of null geodesics and eikonal quasinormal modes [50]. More exactly, the real oscillation frequency is determined by the rotation frequency of the unstable circular null geodesic,[1] and the damping rate is proportional to the Lyapunov exponent [50]. However, as was shown in [54,55], this correspondence works for the WKB-like part of the spectrum and, therefore, is not always guaranteed. Thus, for example, it is not fulfilled for the gravitational perturbations in some theories with higher curvature corrections [14,56].

The other reason to treat separately the eikonal regime is that it may bring qualitatively new features of the perturbations. Thus, for example, the high ℓ modes may govern the instability, called "eikonal instability" [57–60], so that the small ℓ frequencies which are stable in such a case do not have meaning anymore: once there is one unstable mode the system is unstable.

An advantage of the eikonal regime is that it is that rare case in which quasinormal modes can be found analytically,[2] because the WKB method is exact in this limit. Here, we use the general approach and *Mathematica* code shared in [63] in order to find the eikonal formula and some improvement of it via expansion beyond the eikonal limit in powers of $1/\ell$.

The maximum of the effective potential acquires the $1/\kappa^2$ correction,

$$r_{\max} = 3M + \frac{1}{\kappa^2}\left(\frac{r_0}{4} - \frac{M}{3}\right) + \mathcal{O}(1/\kappa^3), \tag{13}$$

where $\kappa = \ell + \frac{1}{2}$. Then expansion in powers of κ gives

$$\omega = \frac{\kappa}{3\sqrt{3}M} - \frac{iK\sqrt{3M - r_0}}{9M^{3/2}} - \frac{36M^2(60K^2 - 29) + 12Mr_0(79 - 156K^2) + r_0^2(492K^2 - 191)}{15552\sqrt{3}M^2\kappa(3M - r_0)} + \mathcal{O}(1/\kappa^2), \tag{14}$$

where $K = n + \frac{1}{2}$.

For the electromagnetic case the effective potential does not gain a r_0 correction, so that the effect is only due to the corrected tortoise coordinate. The terms beyond the eikonal approximation differ from that for the scalar field,

$$\omega = \frac{\kappa}{3\sqrt{3}M} - \frac{iK\sqrt{3M - r_0}}{9M^{3/2}} - \frac{180M^2(12K^2 + 23) - 12Mr_0(156K^2 + 173) + r_0^2(492K^2 + 241)}{15552\sqrt{3}M^2\kappa(3M - r_0)} + \mathcal{O}(1/\kappa^2). \tag{15}$$

For the Dirac field, the maximum of the effective potential is located at

$$r_{\max} = 3M + \frac{\sqrt{M(3M - r_0)}}{2\kappa} + \frac{r_0}{12\kappa^2} + \mathcal{O}(1/\kappa^3), \tag{16}$$

while the quasinormal frequency at the first order in $1/\kappa$ beyond the eikonal limit is

$$\omega = \frac{\kappa}{3\sqrt{3}M} - \frac{iK\sqrt{3M - r_0}}{9M^{3/2}} - \frac{36M^2(60K^2 + 7) - 12Mr_0(156K^2 + 11) + r_0^2(492K^2 + 25)}{15552\sqrt{3}M^2\kappa(3M - r_0)} + \mathcal{O}(1/\kappa^2). \tag{17}$$

[1]It is also worth mentioning that in the nonlinear electrodynamics photons do not move along the null geodesics, so that the terms "null geodesics" and "photons orbits" are not always interchangeable in the correspondence [51–53].

[2]The other examples of spectral problems allowing for an exact solution of the wave equation are mostly for the $2 + 1$ dimensional black holes, such as Banados-Teitelboim-Zanelli space-time and its generalizations [61,62].

TABLE VIII. WKB and time-domain QNMs of the Dirac field for $n = 0$, $k = 1$ and various r_0. The relative errors between the time domain and WKB6(Pade) data are denoted by δ_{Re} and δ_{Im}.

k	r_0	6WKB	6WKB(Pade6)	Time domain	δ_{Re}, %	δ_{Im}, %
1	0	0.366162–0.194105 i	0.365813–0.193991 i	0.363109–0.193879 i	0.7	0.06
1	0.1	0.367621–0.187362 i	0.367360–0.187224 i	0.364974–0.187368 i	0.7	0.08
1	0.2	0.369030–0.180342 i	0.368835–0.180209 i	0.367119–0.181394 i	0.5	0.7
1	0.3	0.370371–0.173012 i	0.370222–0.172915 i	0.368034–0.172499 i	0.6	0.2
1	0.4	0.371617–0.165327 i	0.371491–0.165303 i	0.370519–0.166785 i	0.3	0.9
1	0.5	0.372731–0.157236 i	0.372601–0.157325 i	0.374146–0.157374 i	0.4	0.03
1	0.6	0.373653–0.148676 i	0.373474–0.148926 i	0.374727–0.148994 i	0.3	0.05
1	0.7	0.374286–0.139579 i	0.373987–0.140027 i	0.374984–0.140167 i	0.3	0.1
1	0.8	0.374469–0.129886 i	0.373973–0.130546 i	0.374747–0.130931 i	0.2	0.3
1	0.9	0.373946–0.119604 i	0.373182–0.120470 i	0.373815–0.121222 i	0.2	0.6
1	0.99	0.372613–0.109991 i	0.371527–0.111055 i	0.370985–0.111308 i	0.1	0.2

TABLE IX. WKB and time-domain QNMs of the Dirac field for $n = 0$, $k = 2$ and various r_0. The relative errors between the time domain and WKB6 (Pade) data are denoted by δ_{Re} and δ_{Im}.

k	r_0	6WKB	6WKB(Pade6)	Time domain	δ_{Re}, %	δ_{Im}, %
2	0	0.760077–0.192833 i	0.760073–0.192813 i	0.760131–0.192823 i	0.008	0.005
2	0.1	0.760875–0.186255 i	0.760872–0.186238 i	0.761154–0.185957 i	0.04	0.2
2	0.2	0.761632–0.179435 i	0.761629–0.179421 i	0.761688–0.179197 i	0.008	0.1
2	0.3	0.762336–0.172344 i	0.762334–0.172332 i	0.762438–0.172463 i	0.01	0.08
2	0.4	0.762973–0.164947 i	0.762972–0.164936 i	0.763234–0.164779 i	0.03	0.09
2	0.5	0.763521–0.157200 i	0.763520–0.157189 i	0.763728–0.157047 i	0.03	0.09
2	0.6	0.763948–0.149051 i	0.763947–0.149038 i	0.764161–0.148906 i	0.03	0.09
2	0.7	0.764206–0.140433 i	0.764207–0.140417 i	0.764415–0.140297 i	0.03	0.09
2	0.8	0.764222–0.131264 i	0.764225–0.131243 i	0.764428–0.131139 i	0.03	0.08
2	0.9	0.763872–0.121451 i	0.763878–0.121422 i	0.764084–0.121343 i	0.03	0.07
2	0.99	0.763078–0.111991 i	0.763088–0.111955 i	0.763299–0.111916 i	0.03	0.03

In the eikonal limit the quasinormal frequencies do not depend on the spin of the field under consideration. Comparison of the above formula in the eikonal limit with the Lyapunov exponents and rotational frequency for the null geodesics shows that the null geodesics/eikonal quasinormal mode correspondence is fulfilled in this case.

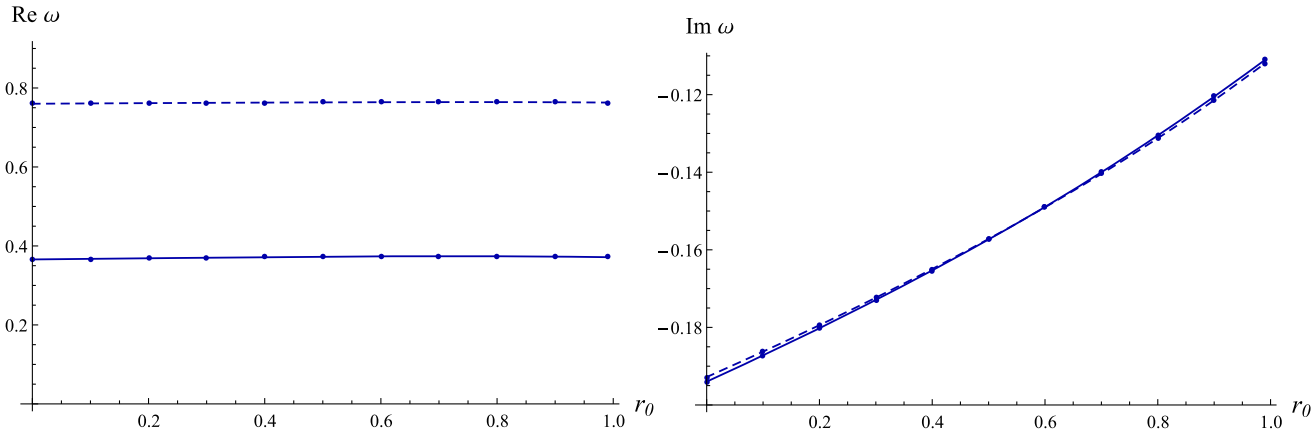

FIG. 8. The modes $n = 0$: $k = 1$ and $k = 2$ (solid and dashed line respectively) for the Dirac field perturbations as functions of r_0.

VIII. CONCLUSIONS

We have presented a detailed study of quasinormal modes of the holonomy-corrected black holes for scalar, electromagnetic and Dirac fields, including the overtones behavior and long-lived modes of a massive field. The quasinormal modes were computed here with two alternative methods (WKB with Padé approximants and Leaver) with excellent agreement between them in the common range of applicability. We have shown that

(1) For a nonzero mass of the field, the quasinormal modes become much longer lived, and there is a clear indication of existence of arbitrarily long-lived modes, i.e., quasiresonances.
(2) The overtones' behavior is in concordance with the observation that the higher the overtone's number, the more it depends on the geometry near the event horizon, while the fundamental mode depends upon the scattering near the peak of the effective potential.
(3) While the third order WKB method used in earlier studies of the holonomy-corrected black hole spectrum agrees well with the Leaver method only at high multipole numbers, application of the sixth order with Padé approximants provides concordance at all ℓ.
(4) The analytical formula for quasinormal modes in the eikonal limit, and at some orders of $1/\ell$ beyond, was deduced, and it may serve as a reasonable approximation for the lowest modes.

The so-called outburst of overtones, which has been studied in a number of works, including for the case of quantum-corrected black holes [64,65], is characterized by a strong deviation of the overtones (already at the first few overtone numbers n) from the Schwarzschild (i.e., nondeformed) case with increasing a deformation parameter, in contrast to the moderate behavior of the fundamental mode. Here we observed a different picture of slow, but still increasing with n, deviation of overtones for both scalar and electromagnetic fields. In principle, the Dirac equation could be rewritten using a different representation basis, so that one could reduce it to the polynomial form [66,67]. Then, the overtones' behavior could be analyzed for the Dirac field as well.

In this paper, we restricted ourselves to the study of the nongravitational case. Calculation of gravitational QNMs in the holonomy-corrected theory can be a subject of separate investigation, including a detailed analysis of the gravitational equations of this theory and their reduction to the wave equation. On the other hand, matter fields usually give a good qualitative representation for the spectrum of gravitational modes (for instance, at large ℓ their spectra are indistinguishable, being close to each other at moderate ℓ).

ACKNOWLEDGMENTS

The author would like to acknowledge Dr. R. A. Konoplya for careful reading of the manuscript and most useful discussions. This work was supported by RUDN University Research Project No. FSSF-2023-0003.

[1] R. A. Konoplya and A. Zhidenko, Quasinormal modes of black holes: From astrophysics to string theory, Rev. Mod. Phys. **83**, 793 (2011).
[2] Emanuele Berti, Vitor Cardoso, and Andrei O. Starinets, Quasinormal modes of black holes and black branes, Classical Quantum Gravity **26**, 163001 (2009).
[3] Kostas D. Kokkotas and Bernd G. Schmidt, Quasinormal modes of stars and black holes, Living Rev. Relativity **2**, 2 (1999).
[4] Hans-Peter Nollert, TOPICAL REVIEW: Quasinormal modes: The characteristic 'sound' of black holes and neutron stars, Classical Quantum Gravity **16**, R159 (1999).
[5] B. P. Abbott *et al.*, Observation of gravitational waves from a binary black hole merger, Phys. Rev. Lett. **116**, 061102 (2016).
[6] B. P. Abbott *et al.*, GW151226: Observation of gravitational waves from a 22-solar-mass binary black hole coalescence, Phys. Rev. Lett. **116**, 241103 (2016).
[7] P. Kanti, R. A. Konoplya, and A. Zhidenko, Quasi-normal modes of brane-localised standard model fields. II. Kerr black holes, Phys. Rev. D **74**, 064008 (2006).
[8] E. Abdalla, B. Cuadros-Melgar, A. B. Pavan, and C. Molina, Stability and thermodynamics of brane black holes, Nucl. Phys. **B752**, 40 (2006).
[9] Sanjeev S. Seahra, Chris Clarkson, and Roy Maartens, Detecting extra dimensions with gravity wave spectroscopy: The black string brane-world, Phys. Rev. Lett. **94**, 121302 (2005).
[10] A. F. Zinhailo, Quasinormal modes of the four-dimensional black hole in Einstein–Weyl gravity, Eur. Phys. J. C **78**, 992 (2018).
[11] R. A. Konoplya, A. F. Zinhailo, and Z. Stuchlik, Quasinormal modes and Hawking radiation of black holes in cubic gravity, Phys. Rev. D **102**, 044023 (2020).
[12] Lorenzo Pierini and Leonardo Gualtieri, Quasi-normal modes of rotating black holes in Einstein-dilaton Gauss-Bonnet gravity: The first order in rotation, Phys. Rev. D **103**, 124017 (2021).
[13] Luciano Manfredi, Jonas Mureika, and John Moffat, Quasinormal modes of modified gravity (MOG) black holes, Phys. Lett. B **779**, 492 (2018).

[14] R. A. Konoplya, A. F. Zinhailo, and Z. Stuchlík, Quasinormal modes, scattering, and Hawking radiation in the vicinity of an Einstein-dilaton-Gauss-Bonnet black hole, Phys. Rev. D **99**, 124042 (2019).
[15] Asier Alonso-Bardaji, David Brizuela, and Raül Vera, Nonsingular spherically symmetric black-hole model with holonomy corrections, Phys. Rev. D **106**, 024035 (2022).
[16] Asier Alonso-Bardaji, David Brizuela, and Raül Vera, An effective model for the quantum Schwarzschild black hole, Phys. Lett. B **829**, 137075 (2022).
[17] A. R. Soares, C. F. S. Pereira, R. L. L. Vitória, and E. Melo Rocha, Holonomy corrected Schwarzschild black hole lensing, Phys. Rev. D **108**, 124024 (2023).
[18] Ednaldo L. B. Junior, Francisco S. N. Lobo, Manuel E. Rodrigues, and Henrique A. Vieira, Gravitational lens effect of a holonomy corrected Schwarzschild black hole, Phys. Rev. D **109**, 024004 (2024).
[19] Guoyang Fu, Dan Zhang, Peng Liu, Xiao-Mei Kuang, and Jian-Pin Wu, Peculiar properties in quasinormal spectra from loop quantum gravity effect, Phys. Rev. D **109**, 026010 (2024).
[20] Zeus S. Moreira, Haroldo C. D. Lima Junior, Luís C. B. Crispino, and Carlos A. R. Herdeiro, Quasinormal modes of a holonomy corrected Schwarzschild black hole, Phys. Rev. D **107**, 104016 (2023).
[21] R. A. Konoplya, Massive vector field perturbations in the Schwarzschild background: Stability and unusual quasinormal spectrum, Phys. Rev. D **73**, 024009 (2006).
[22] Akira Ohashi and Masa-aki Sakagami, Massive quasinormal mode, Classical Quantum Gravity **21**, 3973 (2004).
[23] Matthew Giesler, Maximiliano Isi, Mark A. Scheel, and Saul Teukolsky, Black hole ringdown: The importance of overtones, Phys. Rev. X **9**, 041060 (2019).
[24] Naritaka Oshita, Ease of excitation of black hole ringing: Quantifying the importance of overtones by the excitation factors, Phys. Rev. D **104**, 124032 (2021).
[25] Hideki Ishihara, Masashi Kimura, Roman A. Konoplya, Keiju Murata, Jiro Soda, and Alexander Zhidenko, Evolution of perturbations of squashed Kaluza-Klein black holes: Escape from instability, Phys. Rev. D **77**, 084019 (2008).
[26] R. A. Konoplya and R. D. B. Fontana, Quasinormal modes of black holes immersed in a strong magnetic field, Phys. Lett. B **659**, 375 (2008).
[27] R. A. Konoplya, Magnetic field creates strong superradiant instability, Phys. Lett. B **666**, 283 (2008).
[28] R. A. Konoplya and A. Zhidenko, First few overtones probe the event horizon geometry, arXiv:2209.00679.
[29] R. A. Konoplya, A. Zhidenko, and A. F. Zinhailo, Higher order WKB formula for quasinormal modes and grey-body factors: Recipes for quick and accurate calculations, Classical Quantum Gravity **36**, 155002 (2019).
[30] E. W. Leaver, An analytic representation for the quasi normal modes of Kerr black holes, Proc. R. Soc. A **402**, 285 (1985).
[31] R. A. Konoplya and A. Zhidenko, High overtones of Schwarzschild-de Sitter quasinormal spectrum, J. High Energy Phys. 06 (2004) 037.
[32] Hans-Peter Nollert, Quasinormal modes of Schwarzschild black holes: The determination of quasinormal frequencies with very large imaginary parts, Phys. Rev. D **47**, 5253 (1993).
[33] Alexander Zhidenko, Massive scalar field quasi-normal modes of higher dimensional black holes, Phys. Rev. D **74**, 064017 (2006).
[34] Andrzej Rostworowski, Quasinormal frequencies of D-dimensional Schwarzschild black holes: Evaluation via continued fraction method, Acta Phys. Pol. B **38**, 81 (2007).
[35] Bernard F. Schutz and Clifford M. Will, Black hole normal modes: A semianalytic approach, Astrophys. J. Lett. **291**, L33 (1985).
[36] Sai Iyer and Clifford M. Will, Black hole normal modes: A WKB approach. 1. Foundations and application of a higher order WKB analysis of potential barrier scattering, Phys. Rev. D **35**, 3621 (1987).
[37] R. A. Konoplya, Quasinormal behavior of the d-dimensional Schwarzschild black hole and higher order WKB approach, Phys. Rev. D **68**, 024018 (2003).
[38] Jerzy Matyjasek and Michał Opala, Quasinormal modes of black holes. The improved semianalytic approach, Phys. Rev. D **96**, 024011 (2017).
[39] Yasuyuki Hatsuda, Quasinormal modes of black holes and Borel summation, Phys. Rev. D **101**, 024008 (2020).
[40] Hideo Kodama, R. A. Konoplya, and Alexander Zhidenko, Gravitational stability of simply rotating Myers-Perry black holes: Tensorial perturbations, Phys. Rev. D **81**, 044007 (2010).
[41] S. V. Bolokhov, Black holes in Starobinsky-Bel-Robinson Gravity and the breakdown of quasinormal modes/null geodesics correspondence, arXiv:2310.12326.
[42] S. V. Bolokhov, Long-lived quasinormal modes and oscillatory tails of the Bardeen spacetime, Phys. Rev. D **109**, 064017 (2024).
[43] Carsten Gundlach, Richard H. Price, and Jorge Pullin, Late time behavior of stellar collapse and explosions: 1. Linearized perturbations, Phys. Rev. D **49**, 883 (1994).
[44] Wei-Liang Qian, Kai Lin, Cai-Ying Shao, Bin Wang, and Rui-Hong Yue, On the late-time tails of massive perturbations in spherically symmetric black holes, Eur. Phys. J. C **82**, 931 (2022).
[45] Milena Skvortsova, Quasinormal spectrum of $(2+1)$-dimensional asymptotically flat, dS and AdS black holes, Fortschr. Phys. **72**, 2400036 (2024).
[46] Alexey Dubinsky, Telling late-time tails for a massive scalar field in the background of brane-localized black holes, arXiv:2403.01883.
[47] M. S. Churilova, R. A. Konoplya, Z. Stuchlik, and A. Zhidenko, Wormholes without exotic matter: Quasinormal modes, echoes and shadows, J. Cosmol. Astropart. Phys. 10 (2021) 010.
[48] R. A. Konoplya and A. V. Zhidenko, Decay of massive scalar field in a Schwarzschild background, Phys. Lett. B **609**, 377 (2005).
[49] R. A. Konoplya, A. F. Zinhailo, J. Kunz, Z. Stuchlik, and A. Zhidenko, Quasinormal ringing of regular black holes in asymptotically safe gravity: The importance of overtones, J. Cosmol. Astropart. Phys. 10 (2022) 091.
[50] Vitor Cardoso, Alex S. Miranda, Emanuele Berti, Helvi Witek, and Vilson T. Zanchin, Geodesic stability, Lyapunov exponents and quasinormal modes, Phys. Rev. D **79**, 064016 (2009).

[51] Che-Yu Chen, Mariam Bouhmadi-López, and Pisin Chen, Probing Palatini-type gravity theories through gravitational wave detections via quasinormal modes, Eur. Phys. J. C **79**, 63 (2019).
[52] Che-Yu Chen and Pisin Chen, Eikonal black hole ringings in generalized energy-momentum squared gravity, Phys. Rev. D **101**, 064021 (2020).
[53] Bobir Toshmatov, Zdeněk Stuchlík, Bobomurat Ahmedov, and Daniele Malafarina, Relaxations of perturbations of spacetimes in general relativity coupled to nonlinear electrodynamics, Phys. Rev. D **99**, 064043 (2019).
[54] R. A. Konoplya and Z. Stuchlík, Are eikonal quasinormal modes linked to the unstable circular null geodesics?, Phys. Lett. B **771**, 597 (2017).
[55] R. A. Konoplya, Further clarification on quasinormal modes/circular null geodesics correspondence, Phys. Lett. B **838**, 137674 (2023).
[56] R. A. Konoplya and A. F. Zinhailo, Quasinormal modes, stability and shadows of a black hole in the 4D Einstein–Gauss–Bonnet gravity, Eur. Phys. J. C **80**, 1049 (2020).
[57] Gustavo Dotti and Reinaldo J. Gleiser, Linear stability of Einstein-Gauss-Bonnet static spacetimes. Part I. Tensor perturbations, Phys. Rev. D **72**, 044018 (2005).
[58] Tomohiro Takahashi, Instability of charged Lovelock black holes: Vector perturbations and scalar perturbations, Prog. Theor. Exp. Phys. **2013**, 013E02 (2013).
[59] Tomohiro Takahashi and Jiro Soda, Catastrophic instability of small Lovelock black holes, Prog. Theor. Phys. **124**, 711 (2010).
[60] R. A. Konoplya and A. Zhidenko, The portrait of eikonal instability in Lovelock theories, J. Cosmol. Astropart. Phys. 05 (2017) 050.
[61] Maximo Banados, Claudio Teitelboim, and Jorge Zanelli, The black hole in three-dimensional space-time, Phys. Rev. Lett. **69**, 1849 (1992).
[62] R. A. Konoplya and A. Zhidenko, BTZ black holes with higher curvature corrections in the 3D Einstein-Lovelock gravity, Phys. Rev. D **102**, 064004 (2020).
[63] R. A. Konoplya and A. Zhidenko, Analytic expressions for quasinormal modes and grey-body factors in the eikonal limit and beyond, Classical Quantum Gravity **40**, 245005 (2023).
[64] R. A. Konoplya, Quasinormal modes and grey-body factors of regular black holes with a scalar hair from the effective field theory, J. Cosmol. Astropart. Phys. 07 (2023) 001.
[65] R. A. Konoplya, Z. Stuchlik, A. Zhidenko, and A. F. Zinhailo, Quasinormal modes of renormalization group improved Dymnikova regular black holes, Phys. Rev. D **107**, 104050 (2023).
[66] Hing Tong Cho, Dirac quasinormal modes in Schwarzschild black hole space-times, Phys. Rev. D **68**, 024003 (2003).
[67] H. T. Cho, Alan S. Cornell, Jason Doukas, and Wade Naylor, Split fermion quasi-normal modes, Phys. Rev. D **75**, 104005 (2007).